Structure and Phase Behavior of Block Copolymer Melts near the Sphere−Cylinder Boundary

Ferass M. Abuzaina,[†] Amish J. Patel,[‡] Simon Mochrie,[§] Suresh Narayanan,[⊥] Alec Sandy,[⊥] Bruce A. Garetz,*[,†] and Nitash P. Balsara*[,‡,#]

Othmer Department of Chemical & Biological Sciences & Engineering, Polytechnic University, Brooklyn, New York 11201; Department of Chemical Engineering, University of California, Berkeley, California 94720; Department of Physics, Yale University, New Haven, Connecticut 06520; Argonne National Laboratory, Argonne, Illinois 60439; and Materials Sciences Division and Environmental Energy and Technologies Division, Lawrence Berkeley National Laboratory, University of California, Berkeley, California 94720

Received November 29, 2004; Revised Manuscript Received May 9, 2005

ABSTRACT: The phase behavior of a poly(styrene-*block*-isoprene) copolymer (SI) with styrene volume fraction $f = 0.18$ was studied by small-angle X-ray scattering (SAXS), optical birefringence, and rheology conducted under quiescent conditions and under the influence of shear flow. This sample is located at the border between ordered spheres and ordered cylinders. Near the order−disorder transition, SI block copolymers with $f < 0.18$ form ordered spheres while those with $f > 0.18$ form ordered cylinders. Our sample exhibits a phase transition from ordered cylinders to disordered micelles at 70 ± 2 °C. The cylinder phase obtained by a quiescent quench is highly defective and thus cannot be detected using birefringence. However, birefringence measurements made in the presence of shear flow and high-resolution SAXS measurements on both quiescent and sheared samples confirm the presence of ordered cylinders. The data obtained from our sample differs qualitatively from all previously published data on SI copolymers with $f = 0.18$. We show that the phase behavior, near the sphere−cylinder boundary, depends on all three thermodynamic parameters: f, χ, and N and not just f and χN, as is usually the case. This dependence on f, χ, and N is ascribed to fluctuation effects and the presence of micelles in the disordered phase. By combining the data presented here with previous results in the literature, we estimate the range of compositions over which disordered micelles are obtained in SI copolymer melts.

Introduction

Block copolymers can spontaneously self-assemble into a variety of periodic structures such as spheres on a body-centered-cubic lattice, hexagonally arranged cylinders, etc. At sufficiently high temperatures, entropic factors dominate, and a disordered phase is obtained. In early theoretical work, Helfand and Leibler determined phase behavior of A−B diblock copolymer melts in the strong and weak segregation limits, using f and the product χN as the independent variables.[1,2] Here f is the volume fraction of one of the blocks, χ is the Flory−Huggins interaction parameter between the blocks, and N is the total number of monomers in the block copolymer chain. The results of subsequent studies, both experimental and theoretical, are invariably expressed on χN vs f phase diagrams (e.g., refs 3−5). In other words, the simplification that block copolymer phase behavior is determined by only two parameters (f and χN), and not three parameters (f, χ, and N), appears adequate in most cases.

The experimental methods used to probe the structure of block copolymers include small-angle X-ray scattering (SAXS), small-angle neutron scattering (SANS), transmission electron microscopy (TEM), and optical birefringence (or depolarized light scattering). In most cases, the presence of anisotropic phases such as lamellae and cylinders is more readily detected if macroscopically aligned samples are obtained.[6−9] There is, however, no guarantee that the phases formed in the presence of flow are identical to those formed under quiescent conditions. In fact, flow-induced phase transitions, i.e., the creation of structures under flow that are not observed under quiescent conditions, have been observed in previous experiments.[10−13] All of these flow-induced phase transitions take place in systems near phase boundaries, and the field-induced structures revert to the equilibrium structures after cessation of the flow and sufficient annealing. Application of external fields during microphase separation may, in some cases, facilitate the development of thermodynamically stable (equilibrium) structures from metastable structures.[14,15]

There is a rich body of experimental literature on the phase behavior of weakly ordered diblock copolymers near the sphere-to-cylinder transition. The results obtained by different research groups for polystyrene−polyisoprene (SI) diblock copolymers with polystyrene as the minority component are remarkably consistent.[16−24] Samples near the order−disorder transition with $f < 0.18$ form ordered spheres, while samples with $f > 0.18$ form ordered cylinders. This indicates that the usual independent variables, χN and f, are adequate for describing the phase behavior of these systems. At $f \approx 0.18$, however, samples with different values of N behave differently. An SI diblock copolymer (with $N = 543$, $f = 0.18$) studied in ref 23 exhibited an ordered-cylinder-to-disorder transition, while another SI diblock copolymer (with $N = 870$, $f = 0.18$) studied in ref 24 exhibited two phase transitions: a low-temperature phase transition from ordered cylinders to ordered

[†] Polytechnic University.
[‡] Department of Chemical Engineering, UC, Berkeley.
[§] Yale University.
[⊥] Argonne National Laboratory.
[#] Lawrence Berkeley National Laboratory, UC, Berkeley.
* To whom correspondence should be addressed.

10.1021/ma047540r CCC: $30.25
Published on Web 07/13/2005

spheres and another high-temperature transition from ordered spheres to disorder (N is based on a 100 Å^3 reference volume).

In this paper, we have used SAXS and birefringence under both quiescent and shear flow to study the properties of an SI copolymer with $f \approx 0.18$. The SAXS and birefringence data obtained from this sample are very different from all previous studies on block copolymers. In addition, the phase behavior of this SI copolymer is qualitatively different from the previous two studies on SI copolymers with $f \approx 0.18$.[23,24] We demonstrate the need to go beyond the usual χN vs f phase diagrams to understand the behavior of samples near the sphere−cylinder border. Our results indicate that optical birefringence data from quiescently ordered block copolymers near the sphere−cylinder transition can be misleading.

The effect of concentration fluctuations on the phase behavior of block copolymer melts was first studied by Fredrickson and Helfand.[25] This analysis led to a significant improvement in our understanding of the thermodynamic properties of block copolymer melts.[9] Recent work has led to a clarification of the effect of concentration fluctuations in asymmetric block copolymers. A combination of theoretical and experimental papers has established that the phase that forms upon melting an array of ordered block copolymer spheres is not devoid of structure but is, in fact, composed of disordered micelles.[3,16−20,24,26−31] This is in agreement with theoretical predictions of Semenov.[3] This body of work provides fresh insight into the nature of concentration fluctuations in block copolymers. By combining the data presented here with previous results in the literature, we estimate the range of compositions (f) over which disordered micelles are obtained.

Experimental Details

A polystyrene−polyisoprene diblock copolymer was synthesized by anionic polymerization under high vacuum. The weight-averaged molecular weights of both polystyrene and polyisoprene blocks were determined to be 6.7 and 26.5 kg/mol, respectively, and we refer to this polymer as SI(7−26). We also use this nomenclature to discuss SI samples studied by other groups. The volume fraction of the polystyrene block in SI(7−26), f, is 0.179. Our synthesis and characterization procedures are given in ref 32. Birefringence measurements using a HeNe laser (633 nm wavelength) as the light source were made on 1 mm thick SI(7−26) melts that were first heated to 120 °C to erase the effect of thermal history. The samples, placed between two crossed polarizers, were then quiescently tempered at different temperatures (i.e., 22, 50, 60, and 65 °C) for well over 6000 min, and the total transmitted laser intensity was recorded as a function of time. It took less than 20 min for the sample to reach the final quench temperature after the start of cooling. Time zero is defined as the time when the cooling was started. Reciprocal shear was applied to SI(7−26) using an apparatus described in ref 33. The optic axes of the polarizer and analyzer in the shear experiments were at 45° to the shear flow direction. The sample was first disordered under quiescent conditions at 120 °C and then sheared using a strain amplitude of 200% and a shear plate velocity of 1 mm/s as it was cooled to a final temperature of 50 °C. The shear flow was started immediately at the start of cooling. SAXS data from quiescent SI(7−26) melts were obtained at the 8-ID-I beamline at the Advanced Photon Source (APS) at Argonne National Laboratory, using a thermal history that was similar to that used in the birefringence experiments. Rheological measurements were performed using an ARES rheometer from Rheometric Scientific Inc., with 25 mm parallel steel plates and 1 mm thick sample. The frequency (ω) dependence of the linear viscoelastic shear moduli G' and G'' were measured as a function of decreasing temperature from 100 to 60 °C.

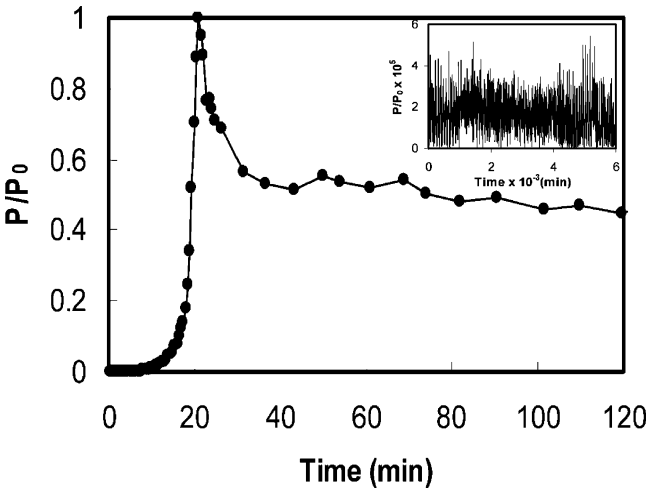

Figure 1. Time dependence of the birefringence signal, P/P_0, of SI(7−26) under shear flow (200% strain amplitude and 1 mm/s shear velocity) at $T = 50$ °C. The inset shows a plot of P/P_0 vs time obtained by quiescently annealing SI(7−26) at 50 °C for several days.

Results

The time dependence of the birefringence signal, P/P_0, where P is the transmitted power and P_0 is the incident power, measured after quiescently quenching SI(7−26) from 120 to 50 °C is shown in the inset of Figure 1. We find that there is no growth of the birefringence signal after quenching. Similar data were obtained after quenches from 120 °C to 22, 60, and 65 °C. Since the sample is located at the sphere−cylinder transition, we only consider the possibility of obtaining ordered spheres, ordered cylinders, and disordered phases. On the basis of a large number of previously published analyses of birefringence data,[12,32−44] we would have concluded that either SI(7−26) was composed of ordered spheres or it was disordered, at temperatures between 22 and 120 °C. We show below that neither of these conclusions is correct.

The time dependence of the birefringence, obtained after quenching SI(7−26) from 120 to 50 °C under reciprocating shear flow, is shown in Figure 1. We find that P/P_0 increases rapidly to unity until $t = 21$ min, then decreases, and levels off. The large birefringence signal indicates the presence of a cylindrical phase under shear flow at 50 °C.

In previous studies we have shown that the cusplike shape of the P/P_0 curve indicates that the retardation of the incident beam exceeds π. The expressions used for interpreting the birefringence data are

$$\frac{P}{P_0} = \sin^2(\Gamma\phi_{sc}/2) \quad \text{for } 0 < \Gamma\phi_{sc} \leq \pi \tag{1}$$

and

$$\frac{P}{P_0} = \sin^2(\pi - \Gamma\phi_{sc}/2) \quad \text{for } \pi \leq \Gamma\phi_{sc} \leq 2\pi \tag{2}$$

where Γ is the retardation of a perfect cylindrically

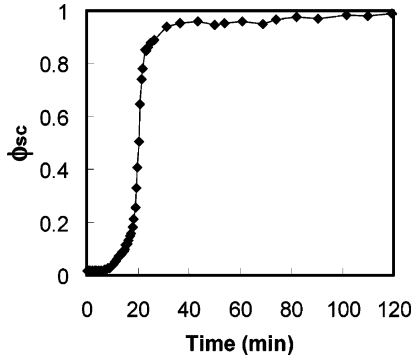

Figure 2. Time dependence of the single-crystal volume fraction, ϕ_{sc}, of SI(7−26) under shear flow (200% strain amplitude and 1 mm/s shear velocity) at $T = 50$ °C.

ordered single-crystal sample with path length L ($\Gamma = 2\pi L\Delta n/\lambda$), Δn is the birefringence of the single crystal, and ϕ_{sc} is the single-crystal volume fraction.

There was no measurable depolarized light scattering at finite scattering angles at any time during the shear flow experiment. On the basis of previous work,[33,36] we take this as an indication that the fraction of randomly oriented grains is either negligible or nearly parallel to the flow direction. Assuming that ϕ_{sc} approaches unity as $t \rightarrow \infty$ when the sample is under high-shear conditions, we estimate that $\Delta n = 4.9 \times 10^{-4}$. This assumption was confirmed qualitatively through reasonable agreement with 4.7×10^{-4}, our estimate of the form birefringence of the sample based on the known refractive indices of polystyrene and polyisoprene, 1.59 and 1.52, respectively. Our estimate does not include intermixing of chains in the microdomains and intrinsic birefringence due to chain stretching.[45] We use our measured value of Δn along with eqs 1 and 2 to compute the time dependence of ϕ_{sc}. The results of the calculation are shown in Figure 2. It is clear that at 50 °C the formation of a cylindrical single crystal takes about 30 min. This is in sharp contrast to the quiescent birefringence results where no sign of order formation was seen for 6000 min (4 days) at 50 °C (inset in Figure 1). The shear aligned state was perfectly stable at room temperature. We were thus able to remove the sample from the shear cell and examine it by SAXS. Standard signatures of oriented, hexagonally packed cylinders were obtained. Since these results were similar to previously published results,[35] we do not show them in this paper.

The shear-oriented sample was heated in steps under quiescent conditions. A discontinuous decrease in the birefringence signal was observed when the sample was heated from 68 to 72 °C. We thus conclude that the cylinders obtained under shear give way to either ordered spheres or disorder at 70 ± 2 °C. We performed a variety of shear experiments, changing shear strain, shearing velocity, and sample temperature. In all cases, we obtained a disordering temperature of 70 ± 2 °C.

SAXS experiments were used to clarify the phase behavior of SI(7−26) melts under quiescent conditions. The sample was disordered at 120 °C, annealed at 50 °C for 48 h in a vacuum, and then taken to the APS. The scattering profile [I vs q, where I is the scattering intensity and q is scattering vector, defined by $q = (4\pi/\lambda)\sin(\theta/2)$, where λ and θ are the wavelength of the incident X-rays and the scattering angle, respectively] obtained at 50 °C is shown in Figure 3. The locations of the higher order peaks at $\sqrt{3}$, $\sqrt{4}$, $\sqrt{7}$, $\sqrt{9}$, and $\sqrt{12}$,

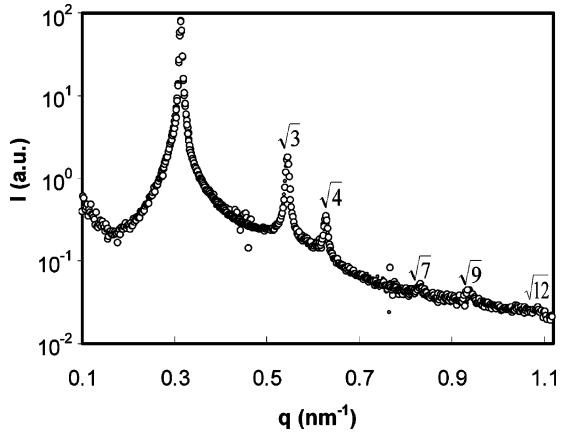

Figure 3. SAXS profile of an extensively annealed SI(7−26) sample at $T = 50$ °C. The relative positions of the higher order scattering peaks are labeled on the profile.

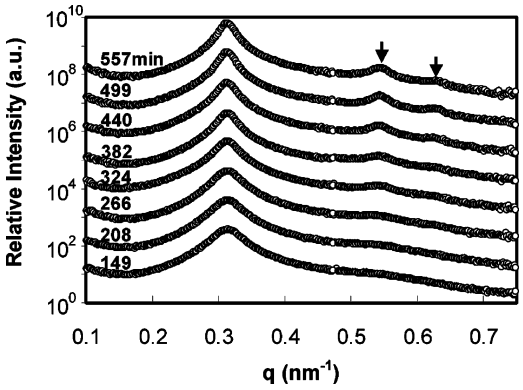

Figure 4. Time evolution of SAXS profiles obtained at 50 °C for SI(7−26); $t = 0$ min is the time at which the cooling of the sample from 70 °C was initiated. The arrows indicate the location of the $\sqrt{3}$ and $\sqrt{4}$ peaks obtained 557 min after quenching the sample.

relative to the primary peak, indicate the presence of hexagonally packed cylinders. The primary peak, located at $q = 0.314$ nm^{-1}, indicates that the intercylinder distance is 23.1 nm, and the cylinder radius is 5.12 nm using the block copolymer composition information. The sample was heated in 10 °C steps. The step from 60 to 70 °C resulted in an abrupt change in the width of the primary SAXS peak and disappearance of the higher order peaks. We thus conclude that the order−disorder transition temperature of SI(7−26) under quiescent conditions is 65 ± 5 °C and that the ordered phase is, in fact, cylindrical. This is in reasonable agreement with the order−disorder transition temperature determined from the birefringence experiments on the aligned sample.

To confirm that the formation of ordered cylinders in SI(7−26) was not caused by the perturbations experienced by the sample while it was transported to the APS, we disordered the sample at 120 °C and cooled the sample in the SAXS instrument in steps of 10 °C. We waited for 57 min at 60 °C (the first step into the ordered state) and found no sign of order formation. Because of limited access to the SAXS instrument, we cooled the sample further to 50 °C (to increase the thermodynamic driving force for order formation) and then held it at that temperature until we saw higher order peaks in the SAXS profiles. In Figure 4 we show data obtained at selected time intervals during the 50 °C experiment. At $t = 557$ min ($t = 0$ min is the time at

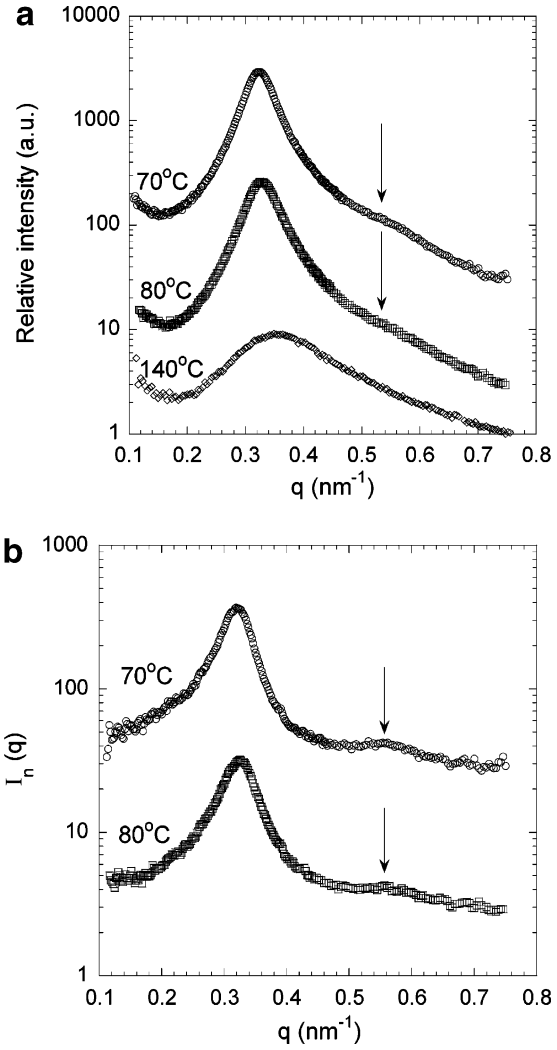

Figure 5. (a) SAXS profiles obtained from SI(7−26) at selected temperatures (70, 80, 140 °C) in the disordered state. (b) A plot of the normalized SAXS intensity $I_N(q)$ at 70 and 80 °C. The arrow indicates the appearance and the location of the broad shoulder that marks the disordered micelles.

which the cooling of the sample from 70 to 60 °C was initiated), the $\sqrt{3}$ and $\sqrt{4}$ peaks of the cylinder phase are evident in the SAXS profiles. Note, however, that 8 h of annealing is needed before signatures of the ordered state are clearly detected in SI(7−26) at 50 °C.

In Figure 5a we show SAXS profiles obtained from SI(7−26) at selected temperatures in the disordered state (70, 80, and 140 °C). The main feature in these scattering profiles is the presence of a peak due to periodic concentration fluctuations at $q = 0.32$ nm^{-1}. To probe the possibility of obtaining disordered micelles, we calculate $I_n(q)$, the $I(q)$ data obtained at the temperature of interest (70 and 80 °C) normalized by that obtained at temperatures deep in the disordered state at 140 °C.[46]

$$I_n(q) = \frac{I(q)_{T°C}}{I(q)_{140°C}} \tag{3}$$

If decreasing the temperature of SI(7−26) melt had led to a simple increase in the amplitude of the concentration fluctuations as proposed by Leibler[2] and Fredrickson and Helfand[25] (i.e., there are no micelles), then $I_n(q)$ would only have a primary peak at $q_{peak} = 0.32$ nm^{-1}

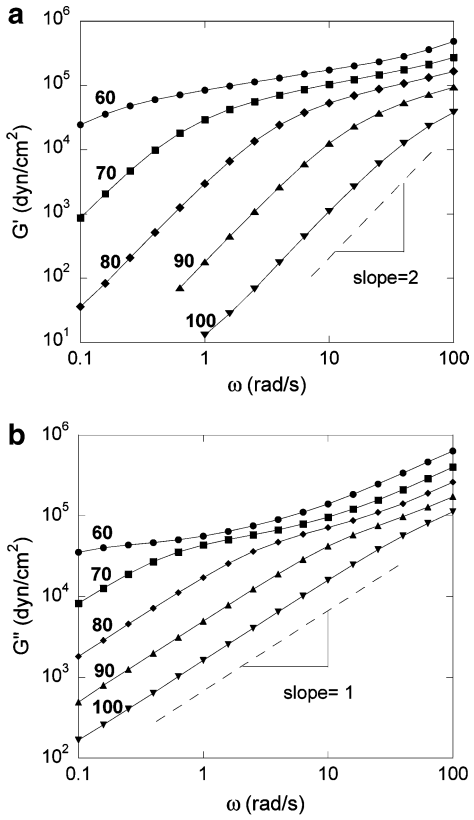

Figure 6. Rheological measurements on SI(7−26) from 60 to 100 °C: (a) in-phase modulus $G'(\omega)$; (b) out-of-phase modulus $G''(\omega)$. For temperatures greater than or equal to 70 °C, terminal behavior is observed.

and no secondary features. This can be readily seen by computing theoretical $I_n(q)$ curves, using the equations given in refs 2 and 25. In Figure 5b we show a plot of $I_n(q)$ at 70 and 80 °C. In addition to the main peak at $q_{peak} = 0.32$ nm^{-1}, we see a broad shoulder around $q = 0.55$ nm^{-1}, as indicated by the arrows in Figure 5b. On the basis of previous reports,[16−20,24,27−31] we propose that this shoulder in $I_n(q)$ indicates the presence of disordered micelles.

To confirm that the high-q SAXS shoulder obtained at 70 and 80 °C was not due to the formation of an ordered phase, we measured the rheological properties of SI(7−26). In Figure 6a,b we plot G' and G'' vs ω.[47] At temperatures greater than or equal to 70 °C we obtain terminal behavior with $G' \sim \omega^2$ and $G'' \sim \omega^1$ in the low-frequency limit. This is a standard signature of a disordered phase.[9] At temperatures less than or equal to 60 °C we obtain significant departures from terminal behavior. For brevity, we only show the 60 °C data in Figure 6. The rheological data support our earlier conclusion based on birefringence and SAXS that the order−disorder transition of this sample is located at 65 ± 5 °C.

Two methodologies have been used to detect the presence of disordered micelles:[16−20,24,27−31] (1) Micellar systems exhibit a high-q ($q > q_{peak}$) shoulder in the disordered state I vs q plots due to the product of the form factor of the spherical cores and the interparticle structure factor.[29] It is has been found, however, that the height of the micelle-related shoulder in the I vs q plot depends on a number of factors such as the magnitude of the concentration fluctuations, the number density of micelles, their aggregation number, etc. Thus, while the presence of a high-q shoulder indicates the

presence of micelles, the absence of a high-q shoulder does not rule out the presence of micelles. (2) The presence of disordered micelles can also be detected by noting the I vs q power law in the high-q limit.[24,27] In the disordered state where the block copolymer chains are mixed at the molecular level, the scattering intensity exhibits a q^{-2} power law at high q, while micellar disordered phases exhibit q^{-4} power law due to Porod scattering from the micellar interfaces.[48] The range of q values where these power laws are observed, however, depends strongly on the magnitude of the concentration fluctuations, the statistical segment lengths of the chains, etc. Unambiguous determination of the high-q I vs q scaling laws requires access to q values that are factors of 4 or 5 higher than the location of the primary scattering peak.[27] Determining the scattering profile at such large q values may not always be feasible due to instrument limitations, background scattering, etc. Our proposal of examining $I_n(q)$ provides a complementary model-free method for identifying the presence of a temperature-dependent micellar regime for cases where the high-q shoulder is not clearly identifiable and SAXS data at very high-q values is not available.

Having established that the ordered phase is in fact cylindrical, we use the quiescent birefringence data (inset of Figure 1) to obtain an upper limit for the average grain size in our system. We start by evaluating the following equation for the depolarized scattered intensity (see ref 38) in the forward direction (as $q \rightarrow 0$):

$$I(q) = \frac{k^4 I_0 V n^2 (n_e - n_o)^2}{15\pi} \int_0^\infty r^2 C(r) \frac{\sin(qr)}{qr} \, dr \quad (4)$$

where the propagation constant $k = 2\pi/\lambda$, λ is the wavelength of the incident beam, I_0 is the incident beam intensity, V is the illuminated sample volume, n is the average refractive index of the medium, and n_e and n_o are the local extraordinary and ordinary refractive indices, respectively. For simplicity, we assume that $C(r)$ is a Gaussian correlation function of the form

$$C(r) = \exp(-r^2/2w^2) \quad (5)$$

Substituting eq 5 in eq 4 at $q = 0$ yields the following expression:

$$\frac{I(0)}{I_0} = \frac{k^4 V n^2 (n_e - n_o)^2 w^3}{15\sqrt{2\pi} L_s^2} \quad (6)$$

where $I(0)$ is the forward scattering intensity, L_s is the sample-to-detection plane (lens location in our setup) distance (150 mm), and w is an average grain length. The ratio $I(0)/I_0$ fluctuates between 0 and about 1.2×10^{-8}, which is near the background noise level of our detection system, for the sample annealed at 50 °C. Using the higher value (1.2×10^{-8}) for the ratio, the average grain length is calculated from eq 6 to be 135 nm. We thus conclude that the average grain length in SI(7−26) after several days of annealing is less than 135 nm due to the complexity of the conversion of disordered micelles into ordered cylinders.

Discussion

Theoretical predictions indicating that the phase behavior of diblock copolymers cannot be determined from f and χN alone are contained in the theoretical work of Fredrickson and Helfand,[25] who proposed a methodology for incorporating fluctuation corrections into Leibler's theory. The phase diagrams obtained by Fredrickson and Helfand were dependent on all three parameters (f, χ, and N). For concreteness, we discuss the theoretical results of Fredrickson and Helfand for a particular value of f ($f = 0.4$). For values of $N < 10^8$, there is a direct transition from disorder to ordered cylinders, while for $N > 10^8$, the disordered phase forms bcc spheres, which then give way to ordered cylinders. The Fredrickson−Helfand approach cannot be implemented for highly asymmetric block copolymers (e.g., $f = 0.18$) because the Hartree analysis, which is the basis for these calculations, is not valid for f values far removed from 0.5.[49]

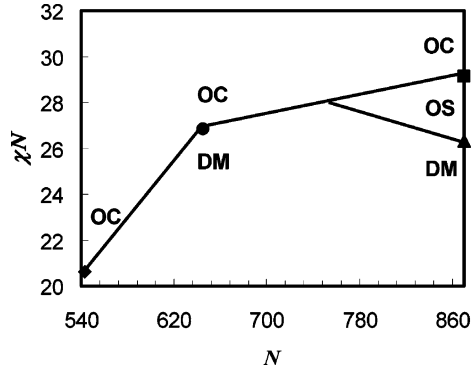

Figure 7. Experimental results shown in a χN vs N plot, for a particular value of f ($f \approx 0.18$), where OC ≡ ordered cylinders, OS ≡ ordered spheres, and DM ≡ disordered micelles. The filled diamond represents sample SI(6−22) from ref 23. The filled square and filled triangle each represent sample SI(9−36) from ref 24. The filled circle represents sample SI(7−26) (present work).

There are some qualitative similarities between the phase behavior observed in SI diblock copolymers with $f \approx 0.18$ and the theoretical predictions of Fredrickson and Helfand. In Figure 7 we show the different phases formed by the $f \approx 0.18$ samples on a χN vs N plot. We used eq 7, proposed by Dormidontova and Lodge[26] for asymmetric SI block copolymers, to calculate χ.

$$\chi = -0.0208 + 21.1/T \quad (7)$$

Both χ and N were based on a 100 Å^3 reference volume. As shown in Figure 7, at $N = 870$, two transitions, from cylinders to spheres and from spheres to disordered micelles, are obtained, as reported in ref 24. When N is decreased to 645, a direct transition from ordered cylinders to disordered micelles is obtained (present work). Similarly, an $N = 543$ sample with $f \approx 0.18$ also shows a cylinder-to-disorder transition as discussed in ref 23. There was no discussion of the nature of the disordered phase in ref 23, which was written before a detailed understanding of the disordered micelle regime was available. On the basis of considerations given in ref 32 and this paper, however, it is likely that the disordered phase at $N = 543$ also contains micelles. The opening of the ordered sphere window at high N in SI diblocks with $f \approx 0.18$ is qualitatively similar to the predictions of Fredrickson and Helfand described in the preceding paragraph. However, the values of N at which we observe changes in phase behavior experimentally are orders of magnitude lower than those indicated by the Fredrickson−Helfand theory. This discrepancy underscores the need for more complete and systematic theories of the phase

behavior of block copolymers, regardless of f. While we have focused on the large differences in N of the polymers discussed in Figure 7, the values of f differ slightly from sample to sample (f of SI(6−22), SI(7−26), and SI(9−36) are 0.188, 0.179, and 0.181, respectively). In our analysis, we have ignored these differences, which are within experimental error.

Our experiments on SI(7−26) indicate that ordered cylinders can be obtained directly by cooling disordered micelles. In previous studies on diblock copolymers, only the formation of ordered spheres from disordered micelles has been reported.[50] It is likely that the mechanism of the transformation from disordered micelles to ordered cylinders is more complicated than the transformation from disordered micelles to ordered spheres. The first step may involve an increase in the number density of the disordered micelles, followed by a conversion of the micelles into wormlike cylinders that eventually are organized on a hexagonal lattice. We propose that our observations of extremely slow ordering, and small grain sizes in quiescently ordered SI(7−26) are due to the complexity of the processes that must occur during the disorder-to-order transition. On the other hand, we find the presence of micelles does not hinder the formation of a well-aligned cylinder phase when shear flow is applied during order formation (Figures 1 and 2).

The presence of disordered micelles also sheds light on complexities noted in early attempts to obtain the χ parameter in polystyrene−polyisoprene block copolymers. In ref 32, the χ parameter between polystyrene and polyisoprene chains was measured by comparing SANS profiles from a series of disordered block copolymers with the theoretical predictions of Leibler.[2] For polymers with $0.25 < f < 0.5$, χ was found to be independent of molecular weight and copolymer composition and was given by

$$\chi = -0.0043 + 13.31/T \tag{8}$$

The agreement of χ obtained from different systems strongly suggests that the disordered phase in systems with $0.25 < f < 0.5$ was devoid of structure (i.e., it did not contain micelles) regardless of N. It was noted in ref 32 that the χ parameters obtained from low molecular weight asymmetric block copolymers with $f < 0.25$ were larger than those obtained from eq 8 by factors as large as 2. The discrepancy was more noticeable at low temperatures near the order−disorder transition than at high temperatures. In no case was χ obtained from the asymmetric systems lower than that given by eq 8. It is now clear anomalously large values of χ obtained from disordered asymmetric block copolymers are signatures of the presence of micelles. (This was one of the explanations offered tentatively in ref 32.) In ref 32 two copolymers, SI(4−13), and SI(8−22), with nearly identical compositions ($f \approx 0.23$) were examined. The χ parameters obtained from SI(8−22) were in agreement with eq 8, while those obtained from SI(4−13) were significantly larger than that predicted by eq 8. We conclude that the disordered phase of SI(4−13) contains micelles while that of SI(8−22) is devoid of structure. It is clear that $f \approx 0.23$ represents the border between structureless disordered phases and micellar disordered phases.

While our understanding of disordered micelles began with the theoretical prediction of Semenov,[3] quantitative understanding of this regime is due to the careful experimentation of several groups[16−20,24,27−31] and more complete theories.[26] Theoretical work of Dormidontova and Lodge shows that as temperature increases, samples in the disordered-micelle regime become increasingly homogeneous. Despite the lack of a sharp discontinuity between the disordered micelle regime and the disordered regime, they were able to determine the temperature at which the concentration of disordered micelles was negligibly small.[26]

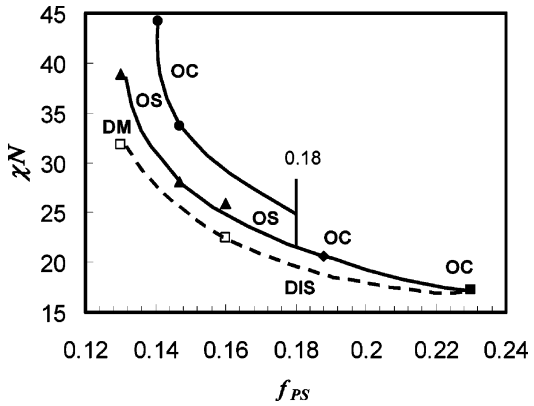

Figure 8. Experimental phase diagram (χN vs f_{PS}) for asymmetric SI block copolymers with PS as the minor component. OC ≡ ordered cylinders, OS ≡ ordered spheres, DM ≡ disordered micelles, and DIS ≡ micelle-free disorder. The filled triangles and the open squares at $f = 0.16$ and $f = 0.13$ correspond to samples SI(7−29) and SI(10−53) from ref 20. The filled circle and the filled triangle at $f = 0.147$ correspond to sample SI(10−50) from ref 17. The filled circle at $f = 0.141$ represents sample SI(14−72) from ref 22. The filled diamond at $f = 0.188$ represents sample SI(6−22) from ref 23. The filled square at $f = 0.23$ represents sample SI(8−22) from ref 32.

The above discussions allow us to plot a refined experimental phase diagram for asymmetric SI block copolymers with polystyrene as the minor component, as shown in Figure 8. Using the data presented here and that in refs 17, 20, 22, 23, and 32, we have identified four kinds of regimes: ordered sphere phase (OS), ordered cylinder phase (OC), disordered micelles (DM), and micelle-free disorder (DIS). The full lines represent phase boundaries. The filled circles represent OC to OS phase transitions identified in refs 17 and 22, while the filled triangles represent the OS to DM phase transitions identified in refs 17 and 20. The vertical line at $f = 0.18$ indicates the inadequacy of the χN vs f format for describing the phase behavior of systems in this region (see Figure 7). There is considerable uncertainty in the location of the ordered sphere and cylinder phases in the $0.15 < f < 0.18$ regime in Figure 8. One source of uncertainty is the fact that the terminus of the sphere−cylinder boundary at $f = 0.18$ will depend on N (Figure 7). In addition, we were unable to find any experimental determination of the sphere−cylinder boundary in the $0.15 < f < 0.18$ regime in the literature. The filled diamond in Figure 8 represents the OC−DM phase transition reported in ref 23, while the filled square represents the OC−DIS phase transition reported in ref 32. The curve connecting the diamond and square is simplistic because the location of the terminus of that curve at $f = 0.23$ depends on N (disordered micelles are obtained at $N = 324$ but not at $N = 582$). The open squares in Figure 8 represent the crossover from disordered micelles to the disordered state reported in ref 20. The dashed curve connects these data (open

squares) with our conclusion that disordered micelles do not exist at $f > 0.23$ (filled square).

Concluding Remarks

The phase behavior of an asymmetric SI diblock copolymer, SI(7−26), was studied by small-angle X-ray scattering and optical birefringence under both quiescent and shear-flow conditions and by rheology. In the absence of shear flow, the sample did not exhibit any measurable birefringence. In the presence of shear flow, however, a well-aligned cylinder phase was obtained. High-resolution SAXS measurements indicated that ordered phase formed under quiescent conditions was cylindrical and that the disordered phase obtained above the order−disorder transition contained micelles. We conclude that the complexity of the conversion of disordered micelles into ordered cylinders results in a highly defective order that cannot be detected by quiescent birefringence experiments. SI(7−26) is the only cylindrical block copolymer sample that we have studied with a negligible quiescent birefringence signal in the ordered state.[41,46,51,52] To our knowledge, this work provides the first evidence of a direct transformation from disordered micelles to ordered cylinders in diblock copolymers.

A significant portion of this paper is devoted to integrating the data obtained from SI(7−26) with the available literature on asymmetric SI block copolymers with polystyrene as the minor component. We present a comprehensive phase diagram obtained from a synthesis of several independent studies.[17,20,22,23,32] For most of the samples we find that the usual parameters χN and f are adequate for describing phase behavior. However, samples with different N values located near the phase boundaries show qualitatively different phase behavior. We suggest that this may be due to the inadequacy of mean-field theories, which include the random phase approximation and self-consistent-field theory.

Given the large number of papers written on block copolymer phase behavior, and the numerous χN vs f phase diagrams that are available in the literature,[2,4,21,25,53−59] one might argue that block copolymer phase behavior is a solved problem. However, our knowledge of these systems is based on a limited number of samples. While the paucity of data in Figure 7 might be considered as a limitation of this work, we are not aware of any asymmetric block copolymer where the thermodynamics of more than three samples with the same value of f have been studied. Given the considerable investment needed to synthesize block copolymers and study their phase behavior as a function of both f and N, our work provides the motivation for more complete studies of systems with $f = 0.18$ and $f = 0.23$.

While this work was under review, a theoretical paper on the formation of disordered micelles in block copolymer melts was published by Wang et al.[60] This work provides considerable support for some of our experimental findings. An important conclusion of ref 60 is that the presence of disordered micelles leads to phase behavior that depends on all three parameters, χ, N, and f. In Figure 7 of ref 60 Wang et al. examine the properties of a block copolymer with $f = 0.10$. At low values of N, they find a direct transition from a disordered micelle phase to an ordered bcc phase. With increasing N, they find that an intermediate face-centered-cubic (fcc) phase is stable between the disordered and bcc phases (Figure 7 of ref 60). This is qualitatively similar to the behavior that we report in Figure 7 of this paper. Quantitative differences arise because Wang et al. did not consider cylinder formation in their study, while in our case we obtain cylinders at $f \approx 0.18$. Despite this, Wang et al. predict that the disordered micelles regime terminates at $f = 0.22$, which is nearly in agreement with our conclusion that this region terminates at $f = 0.23$ (Figure 8). One of our proposed signatures of disordered micelles, namely higher neutron scattering intensity than what is expected from the Leibler structure factor, is shown to be true in theory (Figure 9 of ref 60).

Acknowledgment. Financial support provided by the National Science Foundation (Grants DMR-0213508 and DECS-0103297) and helpful discussions with Glenn Fredrickson are gratefully acknowledged. The APS is supported by the U.S. DOE under Contract W-31-109-Eng-38. We thank Zhen-Gang Wang for providing us with a preprint of ref 60 prior to publication.

References and Notes

(1) Helfand, E. *Macromolecules* **1975**, *8*, 552.
(2) Leibler, L. *Macromolecules* **1980**, *13*, 1602.
(3) Semenov, A. N. *Macromolecules* **1989**, *22*, 2849; *Sov. Phys. JETP* **1985**, *61*, 733.
(4) Matsen, M. W.; Bates, F. S. *Macromolecules* **1996**, *29*, 1901.
(5) Forster, S.; Khandpur, A. K.; Zhao, J.; Bates, F. S.; Hamley, I. W.; Ryan, A. J.; Bras, W. *Macromolecules* **1994**, *27*, 6922.
(6) Folkes, M. J.; Keller. A. *J. Polym. Sci., Polym. Phys. Ed.* **1976**, *14*, 833.
(7) Hadziioannou, G.; Skoulios, A. *Macromolecules* **1982**, *15*, 258.
(8) Koppi, K. A.; Tirrell, M.; Bates, F. S.; Almdal, K.; Colby, R. H. *J. Phys. (Paris)* **1992**, *2*, 1941.
(9) Bates, F. S.; Rosedale, J. H.; Fredrickson, G. H. *J. Chem. Phys.* **1990**, *92*, 6255.
(10) Cates, M. E.; Milner, S. T. *Phys. Rev. Lett.* **1989**, *62*, 1856.
(11) Koppi, K. A.; Tirrell, M.; Bates, F. S. *Phys. Rev. Lett.* **1993**, *70*, 1449.
(12) Balsara, N. P.; Hammouda, B. *Phys. Rev. Lett.* **1993**, *72*, 360.
(13) Jackson, C. L.; Barnes, K. A.; Morrison, F. A.; Mays, J. W.; Nakatani, A. I.; Han, C. C. *Macromolecules* **1995**, *28*, 713.
(14) Park, C.; Simmons, S.; Fetters, L. J.; Hsiao, B.; Yeh, F.; Thomas, E. L. *Polymer* **2000**, *41*, 2971.
(15) Kotaka, T.; Okamoto, M.; Kojima, A.; Kwon, Y. K.; Nojima, S. *Polymer* **2001**, *42*, 1207.
(16) Schwab, M.; Stühn, B. *Phys. Rev. Lett.* **1996**, *76*, 924; *Colloid Polym. Sci.* **1997**, *275*, 341.
(17) Ryu, C. Y.; Lee, M. S.; Hajduk, D. A.; Lodge, T. P. *J. Polym. Sci., Polym. Phys. Ed.* **1997**, *35*, 2811.
(18) Adams, J. L.; Graessley, W. W.; Register, R. A. *Macromolecules* **1994**, *27*, 6026.
(19) Adams, J. L.; Quiram, D. J.; Graessley, W. W.; Register, R. A.; Marchand, G. R. *Macromolecules* **1996**, *29*, 2929.
(20) Han, C. D.; Vaidya, N. Y.; Kim, D.; Shin, G.; Yamaguchi, D.; Hashimoto, T. *Macromolecules* **2000**, *33*, 3767.
(21) Khandpur, A. K.; Foerster, S.; Bates, F. S.; Hamley, I. W.; Ryan, A. J.; Bras, W.; Almdal, K.; Mortensen, K. *Macromolecules* **1995**, *28*, 8796.
(22) Sakurai, S.; Kawada, H.; Hashimoto, T.; Fetters, L. J. *Macromolecules* **1993**, *26*, 5796.
(23) Ogawa, T.; Sakamoto, N.; Hashimoto, T.; Han, C. D.; Baek, D. M. *Macromolecules* **1996**, *29*, 2113.
(24) Kimishima, K.; Koga, T.; Hashimoto, T. *Macromolecules* **2000**, *33*, 968.
(25) Fredrickson, G. F.; Helfand, E. *J. Chem. Phys.* **1987**, *87*, 697.
(26) Dormidontova, E. E.; Lodge, T. P. *Macromolecules* **2001**, *34*, 9143.
(27) Sakamoto, N.; Hashimoto, T.; Han, C. D.; Kim, D.; Vaidya, N. Y. *Macromolecules* **1997**, *30*, 1621.
(28) Harkless, C. R.; Singh, M. A.; Nagler, S. E. *Phys. Rev. Lett.* **1990**, *64*, 2285. Singh, M. A.; Harkless, C. R.; Nagler, S. E.; Shannon, R. F., Jr.; Ghosh, S. S. *Phys. Rev. B* **1993**, *47*, 8425.

(29) Kim, J. K.; Lee, H. H.; Sakurai, S.; Aida, S.; Masamoto, J.; Nomura, S.; Kitagawa, Y.; Suda, Y. *Macromolecules* **1999**, *32*, 6707.
(30) Sakamoto, N.; Hashimoto, T. *Macromolecules* **1998**, *31*, 8493.
(31) Sota, N.; Sakamoto, N.; Saijo, K.; Hashimoto, T. *Macromolecules* **2003**, *36*, 4534.
(32) Lin, C. C.; Jonnalagadda, S. V.; Kesani, P. K.; Dai, H. J.; Balsara, N. P. *Macromolecules* **1994**, *27*, 7769.
(33) Wang, H.; Newstein, M. C.; Chang, M. Y.; Balsara, N. P.; Garetz, B. A. *Macromolecules* **2000**, *33*, 3719.
(34) Wang, H.; Newstein, M. C.; Krishnan, A.; Balsara, N. P.; Garetz, B. A.; Hammouda, B.; Krishnamoorti, R. *Macromolecules* **1999**, *32*, 3695.
(35) Balsara, N. P.; Dai, H. J.; Kesani, P. K.; Garetz, B. A.; Hammouda, B. *Macromolecules* **1994**, *27*, 7406.
(36) Abuzaina, F. M.; Garetz, B. A.; Mody, J. U.; Newstein, M. C.; Balsara, N. P. *Macromolecules* **2004**, *37*, 4185.
(37) Chang, M. Y.; Abuzaina, F. M.; Kim, W. G.; Gupton, J. P.; Garetz, B. A.; Newstein, M. C.; Balsara, N. P.; Yang, L.; Gido, S. P.; Cohen, R. E.; Boontongkong, Y.; Bellare, A. *Macromolecules* **2002**, *35*, 4437.
(38) Garetz, B. A.; Balsara, N. P.; Dai, H. J.; Wang, Z.; Newstein, M. C.; Majumdar, B. *Macromolecules* **1996**, *29*, 4675.
(39) Hahn, H.; Lee, J. H.; Balsara, N. P.; Garetz, B. A.; Watanabe, H. *Macromolecules* **2001**, *34*, 8701.
(40) Newstein, M. C.; Garetz, B. A.; Dai, H. J.; Balsara, N. P. *Macromolecules* **1995**, *28*, 4587.
(41) Perahia, D.; Vacca, G.; Patel, S. S.; Dai, H. J.; Balsara, N. P. *Macromolecules* **1994**, *27*, 7645.
(42) Garetz, B. A.; Newstein, M. C.; Dai, H. J.; Jonnalagadda, S. V.; Balsara, N. P. *Macromolecules* **1993**, *26*, 3151.
(43) Balsara, N. P.; Garetz, B. A.; Dai, H. J. *Macromolecules* **1992**, *25*, 6072.
(44) Balsara, N. P.; Perahia, D.; Safinya, C. R.; Tirrell, M.; Lodge, T. P. *Macromolecules* **1992**, *25*, 3896.
(45) Lodge, T. P.; Fredrickson, G. H. *Macromolecules* **1992**, *25*, 5643.
(46) Hahn, H.; Eitouni, H. B.; Balsara, N. P.; Pople, J. A. *Phys. Rev. Lett.* **2003**, *90*, 155505.
(47) Time−temperature superposition fails on these data, presumably due to the thermorheological complexity of the sample.
(48) Porod, G. *Kolloid Z. Z. Polym.* **1951**, *124*, 83; **1952**, *125*, 51; **1952**, *125*, 108.
(49) Fredrickson, G. H., personal communication.
(50) In ref 31, Sota et al. obtained ordered cylinders directly from disordered spheres when an asymmetric SIS triblock copolymer was deeply quenched below T_{OOT}. Their sample showed two ordered phases (i.e., ordered cylinders and ordered spheres).
(51) Balsara, N. P.; Garetz, B. A.; Newstein, M. C.; Bauer, B. J.; Prosa, T. J. *Macromolecules* **1998**, *31*, 7668.
(52) Newstein, M. C.; Garetz, B. A.; Balsara, N. P.; Chang, M. Y.; Dai, H. J. *Macromolecules* **1998**, *31*, 64.
(53) Forster, S.; Khandpur, A. K.; Zhao, J.; Bates, F. S.; Hamley, I. W.; Ryan, A. J.; Bras, W. *Macromolecules* **1994**, *27*, 6922.
(54) Cho, J. *Macromolecules* **2001**, *34*, 6097.
(55) Floudas, G.; Vazaiou, B.; Schipper, F.; Ulrich, R.; Wiesner, U.; Iatrou, H.; Hadjichristidis, N. *Macromolecules* **2001**, *34*, 2947.
(56) Bates, F. S.; Schultz, M. F.; Khandpur, A. K.; Förster, S.; Rosedale, J. H. *Faraday Discuss.* **1994**, *98*, 7.
(57) Hamley, I. W.; Castelletto, V.; Yang, Z.; Price, C.; Booth, C. *Macromolecules* **2001**, *34*, 4079.
(58) Mai, S.-M.; Fairclough, J. P. A.; Hamley, I. W.; Matsen, M. W.; Denny, R. C.; Liao, B.-X.; Booth, C.; Ryan, A. J. *Macromolecules* **1996**, *29*, 6212.
(59) Schulz, M. F.; Khandpur, A. K.; Bates, F. S.; Almdal, K.; Mortensen, K.; Hajduk, D. A.; Gruner, S. M. *Macromolecules* **1996**, *29*, 2857.
(60) Wang, J.; Wang, Z. G.; Yang, Y. *Macromolecules* **2005**, *38*, 1979.

MA047540R